Indian Journal of Biochemistry & Biophysics
Vol. 60, August 2023, pp. 589-595
DOI: 10.56042/ijbb.v60i8.4293

# Aplastic anemia patients with severe COVID-19 showed abnormal ultrastructure features on type II pneumocytes of lungs

Shikha Chaudhary[1], Ravi P Yadav[1], Shailendra Kumar[2] & Subhash C Yadav[1]*

[1]Electron Microscope Facility, Department of Anatomy; & [2]Department of Anaesthesiology, Pain Medicine and Critical Care, All India Institute of Medical Sciences, New Delhi-110 029, Delhi, India

*Received 22 February 2023*; *revised 14 June 2023*

Type-II-pneumocytes from the bronchoalveolar fluids of aplastic anemia (AA) patients with COVID-19-induced acute respiratory distress syndrome (ARDS) were imaged to assess the ultrastructural alteration, especially in the number and size of the lamellar bodies. The mild (non-ARDS), and severe ARDS without comorbidities were used as reference for comparative ultrastructural analysis. The electron microscopic imaging of mild non-ARDS patients showed normal ultrastructure with surfactant-containing lamellar bodies of size range 0.5-1.00 µM with an area ranging from 0.3-0.8 $\mu M^2$. The ARDS patients with diabetes and without any comorbidities showed larger lamellar bodies of the size range 0.8-1.4 µM with an area range from 0.5-1.50 $\mu M^2$. However, AA patients revealed normal and giant lamellar bodies. These giant lamellar bodies showed a size range of 2.0-4.0 µM with an area ranging from 3.0- 5.0 $\mu M^2$ with a lesser number/cell. This study reports the abnormal ultrastructural alteration of type II pneumocytes in AA patients with COVID-19.

**Keywords**: Pancytopenia, Surfactant granules, Type II pneumocytes

Pancytopenia, (a decrease in all three hematologic cell lines) with bone marrow failure is known as aplastic anemia (AA) with an incidence of two per million population[1]. This is caused by various reasons, such as infections, autoimmune diseases, genetic disorders, nutritional deficiency, and/or malignant conditions. It is clinically described by lower hemoglobin(<12 g/dL in women and <13 g/dL in men), platelets count (<150,000 per mcL), and leukocytes (<4000 per mL), and absolute neutrophil count (<1800 per mL) depending on age, sex, race, and clinical conditions[2]. Many researchers reported the COVID-19-induced pancytopenia-like condition, but it is difficult to establish the pre- or post-manifestation of AA[3]. It has also been reported that pancytopenia was induced by severe acute respiratory syndrome coronavirus 2 (SARS-CoV-2) infection due to cytokine storm and the potential viral cytotoxicity[4,5]. Many researchers reported that patients with minimal respiratory COVID-19 symptoms developed cytopenia and were diagnosed with bone marrow failure. Bone marrow aspiration of these patients showed viral infection and infiltration with SARS-CoV-2[6-9]. The mechanistic link between SARS-CoV-2 infection and bone marrow failure was not effusively reported[10-12]. It was only speculated that SARS-CoV-2 infection-mediated immunologic response was the main reason for bone marrow failure[13].However, very few reports describe the incidence of COVID-19 and its clinical effects on patients already suffering from aplastic anemia[2,14-16]. It was also reported that patients affected by hematological disorders had increased mortality and prolonged viral RNA persistence than patients with non-hematological cancers[17-19]. Avenoso *et al*. studied the impact of SARS-CoV-2 infection on patients already suffering from pancytopenia using a small cohort study of twenty-three aplastic anemia patients and reported the progressive decline in all hematologic indices consistent with overt relapse and requirement of transfusion support. They demonstrated that SARS-CoV-2 infection could jeopardize residual hematopoiesis during aplastic anemia[20]. Another study by Khaled *et al*. reported that AA patients were at higher risk for COVID-19 infection and more prone to develop a severe form of the disease due to immune-deficient conditions[3]. In younger patients without major comorbidities, COVID-19 infection was self-limiting and did not result in AA relapse[14,21]. Considering the finding and clinical outcome studies of AA patients with

*Correspondence:
Phone: +91-11-26549127, +919868126177
Fax: +91-11-26588663/641
E-mail: subhashmbu@aiims.gov.in; subhashmbu@gmail.com

COVID-19 infection, we have investigated the effect of SARS-CoV-2 infection on type II pneumocytes from COVID-19-induced ARDS patients. Patients with mild (mild infection, no ARDS-like condition) and ARDS (without and with comorbidities like diabetes) were used to compare ultrastructural findings similar to the other report[22-24]. We have found abnormal extra-large-size surfactant granules in type II pneumocytes only in patients suffering from aplastic anemia.

## Material and Methods

### Material

Triton X-100 was procured from Fisher Scientific. Osmium tetroxide was procured from Ted Pella, USA. Uranyl acetate was from TAAB, UK, and lead citrate was from Ladd. Karnovsky's fixative (0.5% glutaraldehyde + 2.0 % paraformaldehyde) was purchased from Sigma chemical company, MO, USA.

### Methods

#### *Ethics statement*

BALF of the COVID-19 patients from the Intensive Care Unit (ICU) were collected after taking informed consent from all participants or patient representatives. The study was approved by Institutional Ethics Committee (IEC) (Ref. No. IEC-307/27.04.2020, RP-10/202). We are confirming that all experiments were performed following relevant guidelines and regulations.

#### Study design and sample collection

BALF samples were collected from intubated SARS-CoV-2 positive patients in the COVID-19 intensive care unit (ICU), AIIMS, New Delhi. All samples were collected between 3rd October 2020 and 31st January 2021. The patients were categorized into four groups such as (A) mild infection non-ARDS patients (5 patients), (B) severe infection with ARDS without any comorbidities (5 patients), (C) Severe ARDS patients with diabetes as comorbidities (5 patients) and (D) Severe ARDS patients with pancytopenia before the infection (05 patients) (Fig. 1). RT-PCR test was performed to confirm the COVID-19 infection for all the patients recruited in the study. The ARDS patients were intubated due to hypoxemia ($SpO_2$<90%), high oxygen requirement (flow rate 20-25 L/min), and deteriorating breathing problems.

The BALF (15-20 mL) was primarily fixed in freshly prepared 20 mL, 2X Karnovsky's solution (final 5% glutaraldehyde + 4.0 % formaldehyde) in 0.2 M phosphate buffer. The surface of the sample vials was sterilized with an alcohol/soap solution by incubating for two hours at room temperature and stored at 4°C in a COVID-19-designated refrigerator. The medical records of all patients were reviewed and cross-checked by an on-duty medical physician.

#### Sample processing for the cellular enrichment

After the primary fixation, the BALF solution was diluted ten times with 0.1 M NaCl solution and strained through a nylon mesh cell strainer with a 100 μM pore. The filtrate was centrifuged at 2500 rpm for 3 min in a swinging bucket. The cell pellets were washed 2-3 times for 10 min with PBS solution to remove the excess mucus. The cellular content was enriched by centrifugation at 1200 g for 3 min and resuspended again in the primary fixative A (0.5% glutaraldehyde and 2.0% paraformaldehyde in 0.1M PB buffer). These samples were processed for PAP staining, immunofluorescence (IF), scanning- and transmission electron microscopy (SEM, TEM).

#### Scanning electron microscopy

For SEM, the enriched and primary fixed cellular components of BALF were osmicated, dehydrated with ethanol, critical point dried (E-3100, Quorum Tech), and mounted on double-sided tape on the aluminum stubs. These stubs were sputter-coated with a gold-based sputter coater (HHV BT-150) for 180 sec. Electron micrographs were obtained on EVO18 (Zeiss, Germany) SEM operated at 20 kV accelerating voltage, between 8-10 mm average working distance with SE detector, and magnifications ranging from 5000X to 30000X.

#### Transmission Electron Microscopy

Enriched cellular constituents of BALF were primarily fixed using 2.5% glutaraldehyde + 2.0% paraformaldehyde in 0.1 M phosphate buffer (PB). The fixed cellular pellets were washed with 0.1 M PB (pH 7.4) and secondary-fixed with 1% osmium tetroxide in 0.1 M PB (pH 7.4) for one hour (secondary fixation) at 4°C. Pellets were washed with distilled water for two hours, and en bloc staining was done with 2% uranyl acetate in 50% ethanol. These samples were again washed with distilled water and dehydrated in an ethanol series (50%, 70%, 80%, 90%, and 100%). These pellets were infiltrated and finally embedded in Araldite CY212 resin to prepare the blocks. Resin blocks were trimmed, and 70 nm

ultrathin sections were prepared using UC7 ultramicrotome (Leica). The sections were mounted on grids and stained with 5% uranyl acetate and 5% lead citrate. Cells were imaged using Talos F200 Transmission Electron Microscope (Thermo Fisher Scientific) using a FEG filament operated at 200kV. The size and area of each lamellar body were measured by using ImageJ software.

## Results

In scanning and transmission electron microscopy imaging, type II pneumocytes from the BALF of mild SARS-CoV-2 infected patients (non-ARDS condition) look healthy and have a normal distribution of lamellar bodies of a diameter range of 500-1000nm and area ranging from 0.3-0.8 $\mu M^2$ (Fig. 1). The surface microvilli, mitochondria, and nucleus were well preserved and showed very few virus-like structures in both TEM and SEM images (Fig. 2). However, the patients without comorbidities with SARS-CoV-2 induced ARDS showed an increased number (18±7 per cell section) of lamellar bodies with size ranges 800-1400 nm and area ranging from 0.5-1.50 $\mu M^2$. The cellular ultra-structure, such as the nucleus, mitochondria, and microvilli on the surface, were poorly preserved. Plenty of virus-like structures on the surface of these cells were indicative of severe infection (Fig. 3). The ultrastructure of typeII pneumocytes from COVID-19-induced severe ARDS diabetic patients showed a similar size range, area, and distribution of lamellar bodies like patients without comorbidities (Fig. 4). However, these cells

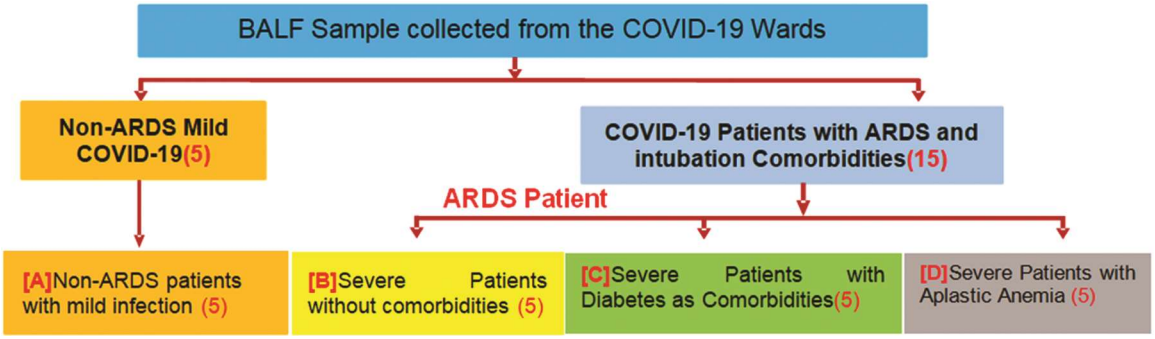


Fig. 1 — Study design to evaluate the effect of SARS-CoV-2 infection on aplastic anemia patients with various controls. The BALF were collected from the intubated patients. The patients were finally grouped under the (A) Non-ARDS, mild infection of SARS-CoV-2 (B) SARS-CoV-2 induced ARDS patients without any comorbidities (C) SARS-CoV-2 induced ARDS patients with diabetes as comorbidities and (D) SARS-CoV-2 induced ARDS patients with aplastic anemia as comorbidities. The mild COVID-19 patients (A) were intubated due to traumatic conditions (not due to COVID-19-induced ARDS) but found COVID-19 positive through RT-PCR. The BALF of these patients were taken to explore the ultrastructural changes of type II pneumocytes between these groups. The number of patients recruited in this study was indicated along with each subgroup

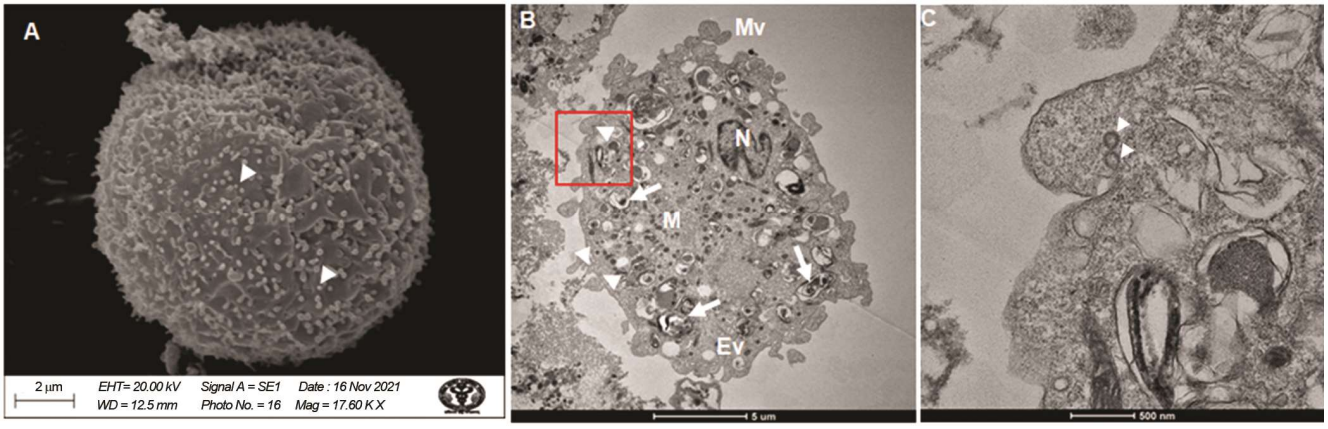


Fig. 2 — Ultrastructural imaging of type II pneumocytes cells from the BALF of mild COVID-19 patients. (A) SEM image of type II pneumocytes cell with regular surface microvilli and very less virus-like structures (white arrowhead); (B)TEM showing irregular surface microvilli (Mv), healthy cell with proper nucleus (N), normal size (0.5-1.0 µM) and area (0.3-0.8 $\mu M^2$) lamellar bodies (white arrow), well-preserved mitochondria (M), and other cell organelles. Very few endocytic vesicles (Ev), and virus-like structure (white arrowhead) were also appreciated; (C) Enlarged view of square area of image B

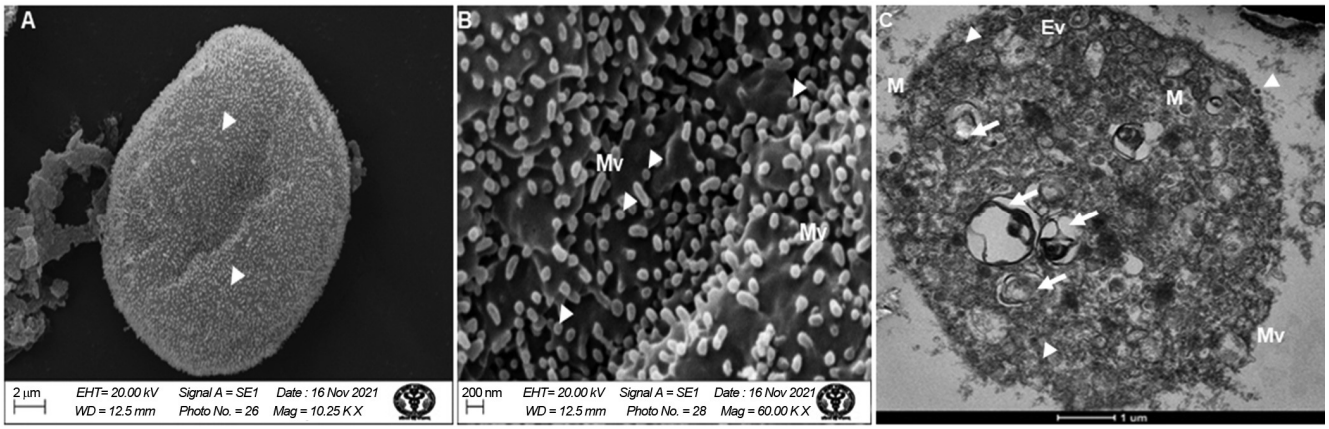


Fig. 3 — Ultrastructural imaging of type II pneumocytes cells from the BALF of severe COVID-19-induced ARDS patients without any comorbidities. (A) SEM image of type II pneumocytes cell with distorted short microvilli and plenty of virus-like structures (white arrowhead); (B) High magnification SEM image with clear distinguishable short microvilli and many SARS-CoV-2 like virus; and (C)TEM image showing a smaller number of irregular and short microvilli (Mv), mitochondria (M), and other cell organelles. Relatively bigger size (800-1250 nm) and higher number (5-8 per cell section) lamellar bodies (white arrow), many endocytic vesicles (Ev), and plenty of SARS-CoV-2 virus-like structures (white arrowhead) were observed

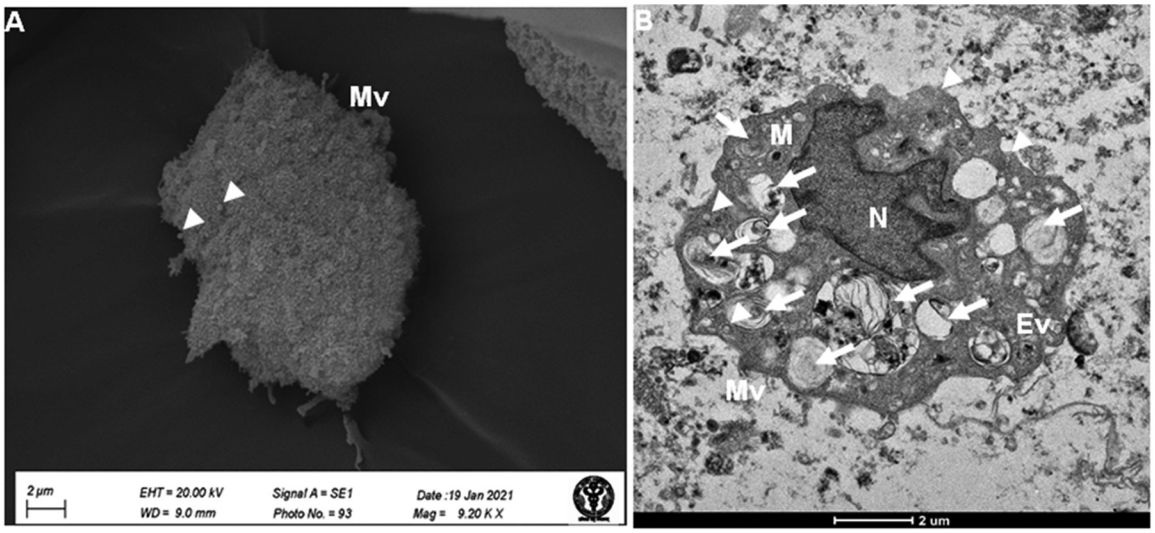


Fig. 4 — Ultrastructural imaging of type II pneumocytes cells from the BALF of severe COVID-19-induced ARDS patients with diabetes.(A) SEM image of type II pneumocytes cell with disintegrating very small size microvilli; and (B) TEM image showing a smooth plasma membrane (very few microvilli, an indication of the high-stress condition), degenerative nucleus (N), very few degenerating mitochondria (M), and other cell organelles. Similar size (800-1400 nm), area (0.5-1.5 $\mu M^2$) and number (8-14 per cell section) of lamellar bodies (white arrow), many endocytic vesicles (Ev), and plenty of SARS-CoV-2 virus-like structures (arrowhead) were observed (like ARDS patients without comorbidities)

from aplastic anemia patients showed two clearly distinguishable size distributions as normal size (<1500 nm diameter) and some giant lamellar bodies (5±2 per cell section) with a size range from 2000-4000nm. The area of smaller lamellar bodies was like other patients (<1.5 $\mu M^2$), but the area of giant lamellar bodies were relatively very high (3.0-5.0 $\mu M^2$). These cells of aplastic anemia patients also showed many mature endocytic viruses, endocytic vesicle formation, enlarged mitochondria, and poor presence of the nucleus (Fig. 5).

## Discussion

The ultrastructural alterations studies of the respiratory tissue/cells from the AA patients after COVID-19 infection may provide cellular insight into the disease. This study was designed to understand the effect of COVID-19 on the ultrastructure of the type II pneumocytes (from BALF) of severe ARDS patients already suffering from aplastic anemia. The severity and lethality of SARS-CoV-2 infection in AA

patients were relatively very high among other comorbidities such as diabetes[3,9,17,18]. To identify the unique ultrastructural changes in type II pneumocytes of AA patients, different control groups, such as non-ARDS (mild infection) and ARDS (without and with comorbidities like diabetes) patients, were recruited in this study (Fig. 1). Type II pneumocytes of the AA patients showed very unusual ultrastructural features, *i.e*., relatively large size lamellar bodies (2000-4000 nm in size and area ranging from 3.0-5.0 $\mu M^2$), called giant lamellar (GL) bodies. However, among the other patient groups, these lamellar bodies showed nearly similar shapes and sizes (Fig. 6). The increase in the size of these lamellar bodies may be attributed to the function of type II pneumocytes. These cells produce alveolar surfactants (to maintain the alveolar and airway stability) that are stored in the lamellar bodies. The nascent lamellar bodies appear to acquire lipids and mature as they move toward the cell's periphery before secretion[25]. The large size lamellar bodies (like the AA patients with COVID-19) were also reported in the Chediak Higashi Syndrome (CHS) with neutropenia, a common characteristic in the aplastic anemia[26].

The number and size of these lamellar bodies gradually increased from mild infection patients to ARDS patients to AA (Fig. 6). The formation of giant lamellar bodies may be due to increased synthesis of surfactants under stress conditions induced by cytokine storms and decreased rate of surfactant release (viral infection). This phenomenon is more prominent in AA patients[27]. Due to the immunocompromised conditions of AA patients, SARS-CoV-2 infection induces very high negative pressure on type II pneumocyte cells compared to

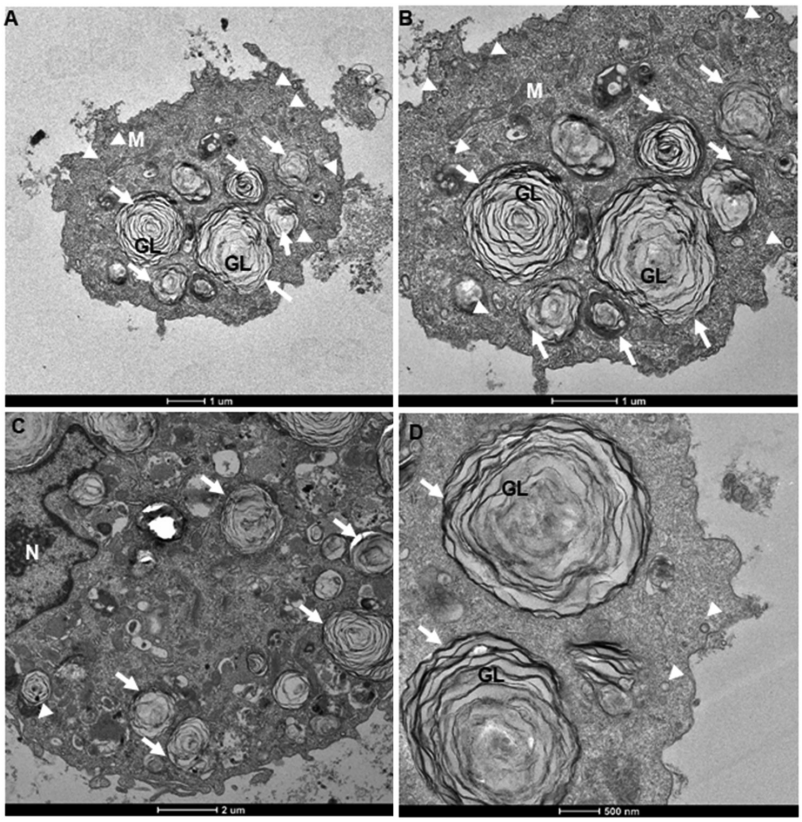


Fig. 5 — Ultrastructural imaging of type II pneumocytes cells from the BALF of severe COVID-19-induced ARDS patients with aplastic anemia.(A) TEM image of type II pneumocytes cell(patient 1) filled with very large and few Giant Lamellar (GL) bodies of size (2.0-4.0 μM ), and area (3.0-5.0 $\mu M^2$). These giant lamellar bodies occupied the maximum cellular space (30-50%). The microvilli (Mv) were nearly absent; thus, these cells were not recognized in the SEM imaging. Plenty of viruses-like structures were seen in the vacuoles and in endocytic vesicles (Ev). Enlarged mitochondria (M) were also observed; (B) High magnification TEM image of (A) with clear, distinguishable giant lamellar bodies, along with normal size lamellar bodies (white arrow), were observed. Cell organelles such as mitochondria (M), endocytic vesicles (Ev) and a few SARS-CoV-2-like viruses (white arrowheads) were clearly visible; and (C & D) magnified view (TEM image) of type II pneumocytes of another COVID-19-infected AA patient (Patient 2). These images showed very few (4-6) giant lamellar bodies, along with 10-15 normal-size lamellar bodies

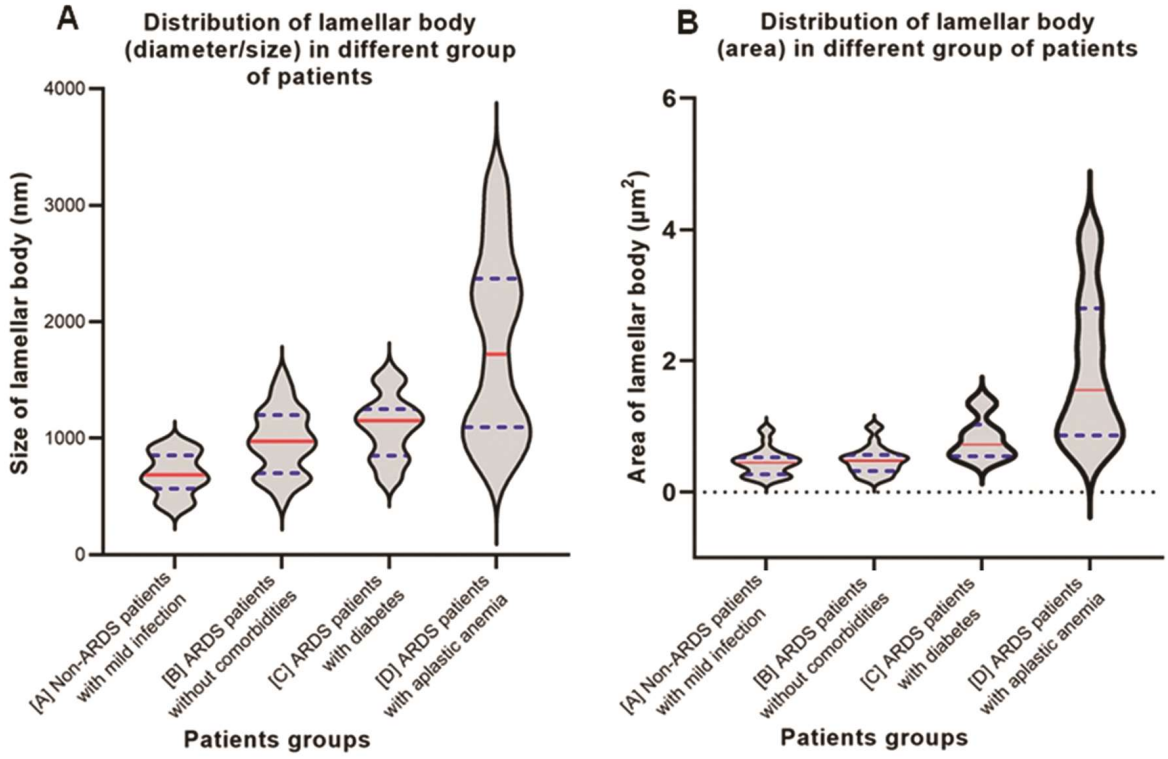


Fig. 6 — Violin plots showing the distribution of lamellar bodies in type II pneumocyte cells from the BALF of different groups of COVID-19 patients. The Violin plots showed the size distribution (A) based on the diameter/size; and (B) based on the area of lamellar bodies. The patient groups are [A] non-ARDS patients with a mild infection (n=5), [B] ARDS patients without comorbidity (n=5), [C] ARDS patients with diabetes (n=5), and [D] ARDS patients with aplastic anemia (n=5). Each violin plot represents the density of lamellar body size distribution for each patient group, with the width of the violin representing the density of lamellar bodies and the red line indicating the median size. The shape of the violin plot reflects the distribution of the data, with narrower sections indicating fewer lamellar bodies and wider sections indicating a higher number of these lamellar bodies. The size of the lamellar bodies was measured from a TEM micrograph with Image J software, and the data were plotted using Prism software. The violin plot suggests that there is a significant difference in the distribution of lamellar body size among the different patient groups. The aplastic anaemia group [D] showed a higher proportion of large lamellar bodies in comparison to the other groups. These findings suggest that the size and distribution of lamellar bodies in type II pneumocytes may be indicative of disease severity and could potentially serve as a diagnostic marker for aplastic anaemia in severe COVID-19 patients

other COVID-19 patients. Reduction in the secretion of surfactant from type II pneumocytes may activate the alveolar macrophage to proliferate and simultaneously infiltrate neutrophils in the alveoli. This infiltration finally leads to the cytokine storm, which could be the reason for the relatively severe effect of COVID-19 on AA patients among other patients in a similar stage of the disease[3,5,7,14,20,21].

## Conclusion

The ultrastructural alteration using scanning and transmission electron microscopy of type II pneumocyte cells from the bronchoalveolar fluids of COVID-19-infected aplastic anemia patients was explored. We have reported abnormal giant lamellar bodies in the type II pneumocytes cells in severely SARS-CoV-2 infected aplastic anemia patients. This report brings new findings to understand the relationship and impact of COVID-19 disease on aplastic anemia patients at the cellular level. The formation of giant lamellar bodies may be due to increased synthesis of surfactants under stress conditions induced by cytokine storms and decreased rate of surfactant release (viral infection).The presence of large giant lamellar bodies in the type II pneumocytes of COVID-19 patients suffering from aplastic anemia is a new finding that suggests a potential disruption in the normal surfactant production and secretion process in the lungs of these patients. This may contribute to the respiratory distress and lung injury observed in severe COVID-19 cases of aplastic anemia patients.

## Acknowledgment

We thank all patients' relatives for permitting us to collect BALF from the patients. This work was supported by grants from the IUSSTF Indo-US Virtual

Network for the COVID-19 program (IUSSTF/VN-COVID/007/2020). Other funding by DBT (BT/INF/22/SP44285/2021), ICMR, SERB, and AIIMS intramural grants is acknowledged. SAIF-AIIMS New Delhi is acknowledged as the imaging facility for the SEM and TEM. DST-FIST confocal microscope facility is also acknowledged for the facility for immunofluorescence. We acknowledged Dr. Kapil Soni and Prof. Anjan Trikha for permission to collect the BALF samples from the respective wards.

## Conflict of interest

All authors declare no conflict of interest.

## References

1 Young NS, Aplastic Anemia. *N Engl J Med*, 379 (2018) 1643.
2 Pawlowski C, Venkatakrishnan AJ, Ramudu E, Kirkup C, Puranik A, Kayal N, Berner G, Anand A, Barve R, O'Horo JC, Badley AD & Soundararajan SV, Pre-existing conditions are associated with COVID-19 patients' hospitalization, despite confirmed clearance of SARS-CoV-2 virus. *EClinicalMedicine*, 34 (2021) 100793.
3 Khaled SA & Hafez AA, Aplastic anemia and COVID-19: how to break the vicious circuit? *Am J Blood Res*, 10 (2020) 60.
4 Dewaele K & Claeys R, Hemophagocytic lymphohistiocytosis in SARS-CoV-2 infection. *Blood*, 135 (2020) 2323.
5 Hersby DS, Do TH, Gang AO & Nielsen TH. COVID-19-associated pancytopenia can be self-limiting and does not necessarily warrant bone marrow biopsy for the purposes of SARS-CoV-2 diagnostics. *Ann Oncol*, 32 (2021) 121.
6 Al-Samkari H, Karp Leaf RS, Dzik WH, Carlson JCT, Fogerty AE, Waheed A, Goodarzi K, Bendapudi PK, Bornikova L, Gupta S, Leaf DE, Kuter DJ & Rosovsky RP, COVID-19 and coagulation: bleeding and thrombotic manifestations of SARS-CoV-2 infection. *Blood*, 136 (2020) 489.
7 Issa N, Lacassin F & Camou F, First case of persistent pancytopenia associated with SARS-CoV-2 bone marrow infiltration in an immunocompromised patient. *Ann Oncol*, 31 (2020) 1418.
8 Kasinathan G & Sathar J, Haematological manifestations, mechanisms of thrombosis and anti-coagulation in COVID-19 disease: A review. *Ann Med Surg (Lond)*, 56 (2020) 56.
9 Tang N, Li D, Wang X & Sun Z, Abnormal coagulation parameters are associated with poor prognosis in patients with novel coronavirus pneumonia. *J Thromb Haemost*,18 (2020) 844.
10 Mohapatra SK & Mukhopadhyay S, Host response to SARS-CoV-2: Insight from transcriptomic studies. *Indian J Biochem Biophys*, 58 (2021) 7.
11 Pandit K, Gupta S & Sharma AG, Clinico-Pathogenesis of COVID-19 in children. *Indian J Biochem Biophys,* 57 (2020) 264.
12 Ray PS & Goswami B, COVID-19 and Hyperinflammatory Syndrome. *Indian J Biochem Biophys,* 57 (2020) 662.
13 Lee NCJ, Patel BA, Bat T, Ibrahim IF, Vusirikala M, Chen M, Rosado FG, Jaso J, Young NS & Chen W, Sars-Cov-2 Infection Associated with Aplastic Anemia and Pure Red Cell Aplasia. *Blood*, 138 (2021) 2195.
14 Paton C, Mathews L, Groarke EM, Rios O, Lotter J, Patel BA & Young NS, COVID-19 infection in patients with severe aplastic anaemia. *Br J Haematol*, 193 (2021) 902.
15 Pathak M, Quantitative analysis of international collaboration on COVID-19: Indian perspective *Indian J Biochem Biophys*, 57 (2020) 439.
16 Parchwani D, Trivedi D, Bhatt A, Dholariya S, Chaudhari SP & Pathak M, Global research trends of interleukin-6 in SARS-CoV-2 infection. *Indian J Biochem Biophys*, 59 (2022) 528.
17 Shah V, Ko Ko T, Zuckerman M, Vidler J, Sharif S, Mehra V, Gandhi S, Kuhnl A, Yallop D, Avenoso D, Rice C, Sanderson R, Sarma A, Marsh J, de Lavallade H, Krishnamurthy P, Patten P, Benjamin R, Potter V, Ceesay MM, Mufti GJ, Norton S, Pagliuca A, Galloway J & Kulasekararaj AG, Poor outcome and prolonged persistence of SARS-CoV-2 RNA in COVID-19 patients with haematological malignancies; King's College Hospital experience. *Br J Haematol*. 190 (2020) e279.
18 Yang X, Yu Y, Xu J, Shu H, Xia J, Liu H, Wu Y, Zhang L, Yu Z, Fang M, Yu T, Wang Y, Pan S, Zou X, Yuan S & Shang Y, Clinical course and outcomes of critically ill patients with SARS-CoV-2 pneumonia in Wuhan, China: a single-centered, retrospective, observational study. *Lancet Respir Med*, 8 (2020) 475.
19 Zhu N, Zhang D, Wang W, Li X, Yang B, Song J, Zhao X, Huang B, Shi W, Lu R, Niu P, Zhan F, Ma X, Wang D, Xu W, Wu G, Gao GF & Tan W, A Novel Coronavirus from Patients with Pneumonia in China, 2019. *N Engl J Med*, 382 (2020) 727.
20 Avenoso D, Marsh JCW, Potter V, Pagliuca A, Slade S, Dignan F, Tholouli E, Mittal S, Davis B, Tauro S, Kesse-Adu R, Griffin M, Payne E, Gandhi S & Kulasekararaj AG, SARS-CoV-2 infection in aplastic anemia. *Haematologica*, 107 (2022) 541.
21 Keiffer G, French Z, Wilde L, Filicko-O'Hara J, Gergis U & Binder AF, Case Report: Tocilizumab for the Treatment of SARS-CoV-2 Infection in a Patient With Aplastic Anemia. *Front Oncol*, 10 (2020) 562625.
22 Chaudhary S, Rai P, Joshi A, Yadav P, Sesham K, Kumar S, Mridha AR, Baitha U, Nag TC, Soni K, Trikha A & Yadav SC, Ultracellular imaging of bronchoalveolar lavage from young age COVID-19 patients with comorbidities showed greater SARS-COV-2 infection but lesser ultrastructural damage than the old age patients. *Microsc and Microanal*, 28 (2022) 2105.
23 Chaudhary S, Rai P, Sesham K, Kumar S, Singh P, Nag TC, Chaudhuri P, Trikha A & Yadav SC, Microscopic imaging of bronchoalveolar fluids of COVID-19 positive intubated patients reveals the different level of SARS-CoV-2 infection on oral squamosal epithelial cells. *Indian J Biochem Biophys*, 58 (2021) 196.
24 Chaudhary S, Yadav RP, Kumar S & Yadav SC, Ultrastructural study confirms the formation of single and heterotypic syncytial cells in bronchoalveolar fluids of COVID-19 patients. *Virol J*, 20 (2023) 97.
25 Fisher AB, Lung lipid composition and surfactant biology. In: Parent RA, ed. *Comparative Biology of the Normal Lung*. London: Christine Minihane; (2015) 423.
26 Chi EY, Prueitt JL & Lagunoff D, Letters to the Editor: Abnormal lamellar bodies in type II pneumocytes and increased lung surface active material in the beige mouse. *J Histochem Cytochem*, 23 (1975) 863.
27 Fehrenbach H, Brasch F, Uhlig S, Weisser M, Stamme C, Wendel A & Richter J, Early alterations in intracellular and alveolar surfactant of the rat lung in response to endotoxin. *Am J Respir Crit Care Med*, 157 (1998) 1630.